Inorganic Chemistry

Article

pubs.acs.org/IC

Electronic Structure of Six-Membered N-Heterocyclic Carbenes and Its Heavier Analogues: Reactivity of the Lone Pair versus the Exocyclic Double Bond

Vallyanga Chalil Rojisha, Susmita De, and Pattiyil Parameswaran*

Department of Chemistry, National Institute of Technology Calicut, Kozhikode, Kerala, India−673 601

Supporting Information

ABSTRACT: Electronic structure of the six-membered N-heterocyclic carbene, silylene, germylene, and stannylene having an exocyclic double bond at the C3 carbon atom as well as the relative reactivity of the lone-pair on the divalent group 14 element and the exocyclic double bond have been studied at the BP86 level of theory with a TZVPP basis set. The geometrical parameters, NICS values, and NBO population analysis indicate that these molecules can be best described as the localized structure $\mathbf{1X}_a$, where a *trans*-butadiene (C1−C2−C3−C4) unit is connected with diaminocarbene (N1−X−N2) via N-atoms having a little contribution from the delocalized structure $\mathbf{1X}_b$. The proton affinity at X is higher than at C4 for **1C**, and a reverse trend is observed for the heavier analogues. Hence, the lone pair on a heavier divalent Group 14 element is less reactive than the exocyclic double bond. This is consistent with the argument that, even though the parent six-membered carbene and its heavier analogues are nonaromatic in nature, the controlled and targeted protonation can lead to either the aromatic system **3X** having a lone pair on X or the nonaromatic system **2X** with readily polarizable C3−C4 π-bond. The energetics for the reaction with BH_3 and $W(CO)_6$ further suggest that both the lone pair of Group 14 element and the exocyclic double bond can act as Lewis basic positions, although the reaction at one of the Lewis basic positions in **1X** does not considerably influence the reactivity at the other. The protonation and adduct formation with BH_3 and $W(CO)_5$ at X lead to nonaromatic systems whereas similar reactions at C4 lead to aromatic systems due to π-bond polarization at C3−C4. The degree of polarization of the C3−C4 π-bond is maximum in the protonated adduct and reduces in the complexes formed with BH_3 and $W(CO)_5$.

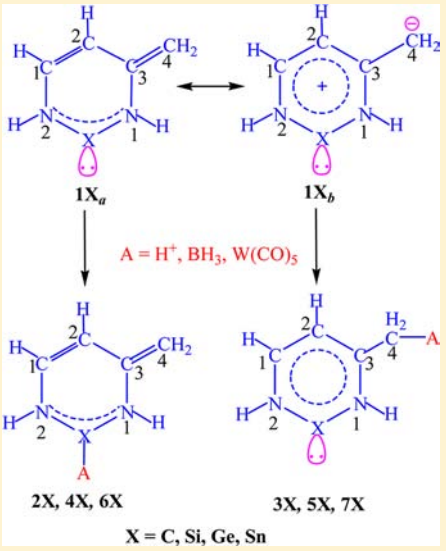

INTRODUCTION

Ever since their detection as transient intermediates, carbenes are realized as important reagents in organic, inorganic, and organometallic chemistry.[1] The first successful isolation of stable singlet carbene $C[PR_2][Si(CH_3)_3]$ (R = diisopropylamino) has been reported by Bertrand and co-workers in 1988.[2a−c] However, the significant role of singlet carbenes in chemistry has been marked by the synthesis of first N-heterocyclic carbene (NHC) in 1991 by Arduengo and co-workers.[2c,d] Here, the carbene carbon atom is flanked between two N atoms in a five-membered heterocycle (NHC) (see Scheme 1, **i**). The cyclization and aromatic stability in the ring structure contributed significantly to the stability of singlet carbenes. The characterization of stable NHC was followed by the isolation of heavier five-membered silylene,[3] germylene,[4] stannylene,[5] and plumbylene[6] analogues. However, the chemistry of NHCs[1] have been developed tremendously, compared to their heavier analogues.[3−7] Despite the advances, the examples of stable NHCs are largely limited to aromatic and saturated cyclic five-membered singlet carbenes.[1j−n] Therefore, the synthesis of other cyclic NHCs with different number of atoms in the ring and different electronic structure is of immense interest.

The reports of six-membered carbenes are limited in literature, compared to five-membered carbenes.[8] Reports of the six-membered carbene with perimidine skeleton (Scheme 1, **ii**) by Richeson and co-workers,[8a] carbene analogues of borazine (Scheme 1, **iii**) by Bertrand and co-workers,[8b] and the six-membered N-heterocyclic carbanions with B-atoms adjacent to N-atoms (Scheme 1, **iv**) by Roesler and co-workers[8c] are the notable six-membered aromatic carbenes. Apart from these aromatic systems, the saturated six-membered carbenes are also reported (Scheme 1, **v**).[8d−g] However, the simplest six-membered unsaturated N-heterocyclic carbene similar to Arduengo's carbene would be an open-shell species with 7π electrons. Nevertheless, the introduction of an exocyclic double bond at one of the noncarbene carbon atoms in the ring might lead to a stable singlet carbene, consisting of a cyclic system with 6π electrons by imparting

Received: April 21, 2012
Published: July 17, 2012

   dx.doi.org/10.1021/ic300821r | *Inorg. Chem.* 2012, 51, 8265−8274

Scheme 1. Schematic Representation of Experimentally Reported N-Heterocyclic Carbenes (i–vii)

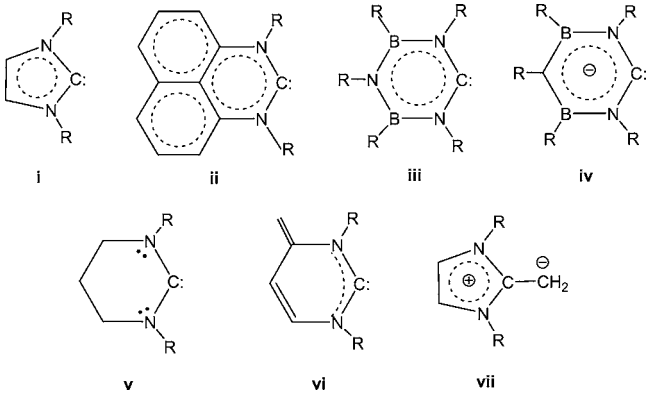

polarization of the exocyclic double bond (Scheme 1, **vi**). In this context, it is worth mentioning that Rivard and co-workers reported the five-membered N-heterocyclic olefins, which show high nucleophilic character at the exocyclic CH_2 group (Scheme 1, **vii**).[7d] Although such six-membered N-heterocyclic carbenes are not yet synthesized, the unexpected synthesis and unusual reactivities of silylene[9] and germylene[10] analogues are undoubtedly remarkable. The reactivity study of the six-membered silylene using muon spectroscopy by Percival and co-workers identified two dominant reactive sites for free-radical attack, viz., the Si atom and the exocyclic methylene carbon.[11a] Driess and co-workers reported betain-type reactivity for germylene with Me_3SiOTf and 1,2-dibromoethane.[10a] Similar 1,4-insertion reactions with other reactants are also reported for both the six-membered silylene[9,11b] and germylene.[10b,12] Density functional calculations by Veszprémi and co-workers suggest that the six-membered carbenes, silylenes, and germylenes are nonaromatic and kinetically stable toward dimerization.[13] There are a few theoretical studies on six-membered ring carbene and its heavier analogues discussing about the stability and substituents effects.[14] However, the detailed understanding of the electronic structure and reactivity of the six-membered N-heterocyclic carbene and its heavier analogues are lacking.

Herein, we have undertaken the structure, bonding, and reactivity study of six-membered N-heterocyclic carbene and its heavier analogues, **1X**, where X = C, Si, Ge, and Sn. $\mathbf{1X}_a$ and $\mathbf{1X}_b$ indicate two important resonating structures (see Scheme 2). Note that $\mathbf{1X}_a$ is a nonaromatic localized structure and $\mathbf{1X}_b$ is a delocalized structure with polarized exocyclic C3–C4 double bond. Hence, there are two major nucleophilic centers, viz., the lone pair on X and the exocyclic double bond, which are not a part of the aromatic delocalization in the six-membered ring. The comparative study of the reactivity of these two nucleophilic centers is focused in the current study. The reluctance of the heavier elements to undergo sp hybridization[15] would also influence the relative stability of these resonating structures and that, in turn, will affect their reactivity as a ligand. In order to investigate their ligand property, protonation and adduct formation with BH_3 and $W(CO)_5$ at X and at C4 were explored.

COMPUTATIONAL METHODOLOGY

The geometries of all molecules were optimized at the nonlocal DFT level of theory using the exchange functional of Becke in conjunction with the correlation functional of Perdew (BP86).[16] The basis sets have triple ζ-quality augmented by two sets of polarization functions (def2-TZVPP).[17] This level of theory is denoted as BP86/TZVPP. The nature of the stationary points on the potential energy surface has been verified by calculating the Hessian matrices analytically.[18] The calculations were carried out with the Gaussian 09 program package.[19] Natural bond order (NBO)[20] and nucleus-independent chemical shifts (NICS)[21] by employing the gauge-invariant atomic orbital[22] (GIAO) approach were computed at the same level of theory. The more-reliable indicator for aromaticity, $NICS_{zz}$, which is the component perpendicular to the ring plane of the NICS tensor, was also calculated. The NICS values are further verified using a more diffuse function containing basis set def2-TZVPPD.[23] Single-point calculations on the BP86/TZVPP optimized geometries of **1X**, **2X**, **3X**, and

Scheme 2. Schematic Representation of the Resonating Structures of 1X (X = C, Si, Ge, and Sn) and Its Reactions with H^+, BH_3, and $W(CO)_6$

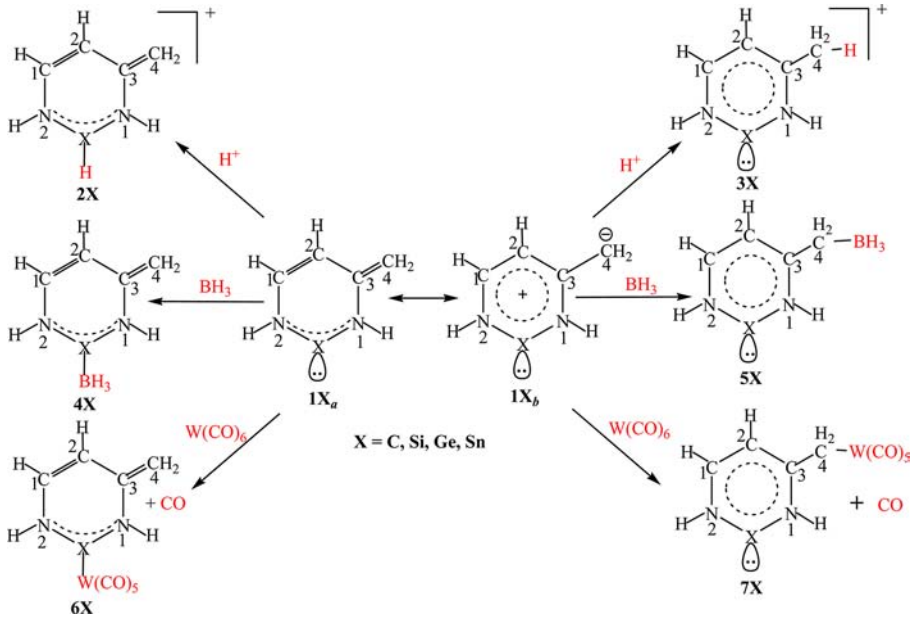

dx.doi.org/10.1021/ic300821r | Inorg. Chem. 2012, 51, 8265–8274

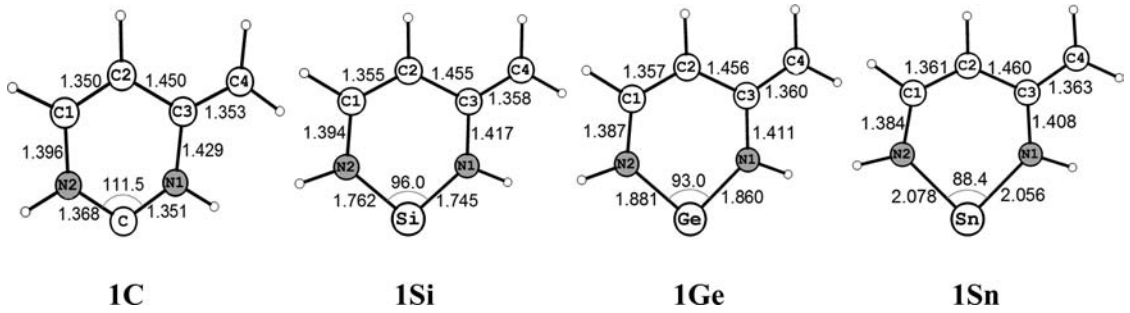

Figure 1. Optimized geometries (BP86/TZVPP) and important geometrical parameters of **1X** (X = C, Si, Ge, and Sn). Distances are given in Ångstroms, angles are given in degrees.

Table 1. Selected Wiberg Bond Orders, Charge Distribution Given by the Natural Population Analysis, and NICS Values for 1X at the BP86/TZVPP Level of Theory

1X	P(C1−C2)[a]	P(C2−C3)[a]	P(C3−C4)[a]	q(X)[b]	q(C3)[b]	q(C4)[b]	q(CH_2)[b]	s(X)[c]	p_z(X)[c]	p_x(X)[c] (p_y(X))	NICS(0)[d] (NICS(0)$_{zz}$)	NICS(1)[d] (NICS(1)$_{zz}$)
1C	1.73	1.13	1.73	0.13	0.09	−0.50	−0.09	1.27	0.57	1.15 (0.83)	5.1 (30.5)	1.6 (7.2)
1Si	1.72	1.13	1.71	1.01	0.11	−0.50	−0.10	1.59	0.33	0.62 (0.40)	4.4 (27.4)	2.2 (8.3)
1Ge	1.70	1.12	1.70	1.03	0.10	−0.52	−0.12	1.71	0.34	0.64 (0.26)	5.4 (31.5)	2.9 (10.9)
1Sn	1.69	1.12	1.68	1.09	0.10	−0.53	−0.13	1.78	0.33	0.54 (0.24)	6.2 (34.2)	3.8 (14.2)

[a]**P** represents bond orders. [b]**q** represents charge on an atom or group of atoms. [c]$s(X)$, $p_z(X)$, $p_x(X)$, and $p_y(X)$ represent partial occupancies in the respective atomic orbitals of atom X. [d]NICS(0) and NICS(1) represent NICS values at the center of the ring and 1 Å above. The dissected NICS(0)$_{zz}$ and NICS(1)$_{zz}$ are given in the parentheses.

8X have also been carried out using meta-GGA exchange correlation functional M06[24] with TZVPP basis set. The energies at M06/TZVPP level were corrected by adding the zero-point energies from the BP86/TZVPP level of theory. The variations in the calculated proton affinities are within ±3 kcal/mol; hence, we limit our discussion at the BP86/TZVPP level of theory, unless otherwise specified.

RESULTS AND DISCUSSION

Structure and Bonding Analysis of 1X. The optimized geometries of the six-membered carbene and its higher analogues are shown in Figure 1. All structures are planar with the exocyclic CH_2 group at C3 lying in the same plane as that of the six-membered ring. The C3−C4 bond distances are close to standard C═C bond distances. The geometrical parameters for C1−C2−C3−C4 skeleton are similar to that of *trans*-butadiene at the same level of theory.[25] The N1−X−N2 bond angle reduces from 111.5° when X = C to 88.4° when X = Sn, because of the increasing size of X. However, the geometrical changes do not have a significant effect on the butadiene unit. These geometrical parameters are consistent with the DFT calculations by Veszprémi and co-workers.[13] The structures with CH_2 group perpendicular to the six-membered ring converge into planar geometries upon optimization. Hence, the resonating structure **1X**$_b$ with completely polarized C3−C4 π-bond is unstable.

The NICS calculations[21] were performed at the center, NICS(0) and NICS(0)$_{zz}$ and 1 Å above the center of the six-membered ring, NICS(1) and NICS(1)$_{zz}$ (see Table 1) for these molecules. A basis set with diffuse functions def2-TZVPPD is used to verify these NICS values on **1X** (see Table S4 in the Supporting Information); however, the calculated NICS values do not vary significantly.[21d] Hence, the NICS values at BP86/TZVPP level are discussed. The close-to-zero NICS values indicate the nonaromatic nature of **1X**, as concluded by the earlier theoretical calculations.[13] The NICS(0) values for the five-membered N-heterocyclic carbene, silylene, and germylene are −12.9, −10.1, and −10.1, respectively, at the B3LYP/6-31+G* level of theory.[26] A small increment in the NICS values is noted when X changes from C to Sn. However, the highly positive NICS$_{zz}$ values indicate a large paratropic ring current perpendicular to the ring. Note that NICS(0)$_{zz}$ and NICS(1)$_{zz}$ values for benzene are −15.7 and −28.9, respectively, at the same level of theory. Thus, the most contributing resonance structure would be the localized structure **1X**$_a$, rather than the aromatic structure **1X**$_b$. This indicates that the stabilization gained from aromaticity is not enough to compensate the destabilization from the polarization of C3−C4 π-bond. Hence, the geometrical and NICS analysis suggest that the six-membered N-heterocyclic carbene and its heavier analogues can be best described as a diaminocarbene (or its heavier analogues) unit connected to a butadiene unit via N-atoms and the most contributing resonance structure is **1X**$_a$ (see Scheme 2).

The important molecular orbitals (MO) of **1C** are plotted in Figure 2. The HOMO−LUMO gap of **1X** is slightly less than that of the corresponding five-membered NHC at the same level of theory.[27] The HOMO of **1C** is a π−MO mainly located

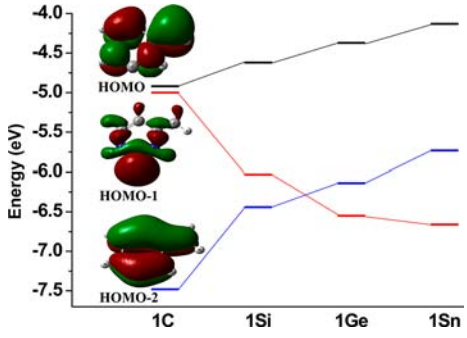

Figure 2. Plot of important molecular orbitals of **1C** and the correlation diagram connecting the molecular orbitals of **1C**, **1Si**, **1Ge**, and **1Sn**.

dx.doi.org/10.1021/ic300821r | Inorg. Chem. 2012, 51, 8265−8274

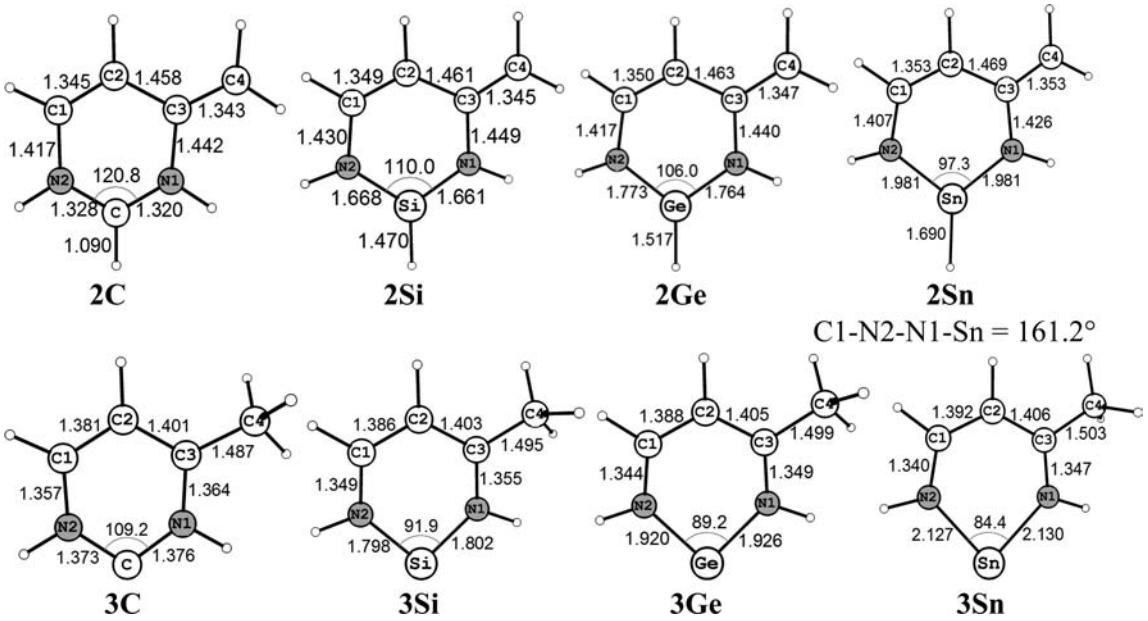

Figure 3. Optimized geometries (BP86/TZVPP) and important geometrical parameters of **2X** and **3X** (X = C, Si, Ge, and Sn). Distances are given in Ångstroms, angles are given in degrees.

Table 2. Calculated Reaction Energies of 1X at the BP86/TZVPP and M06/TZVPP//BP86/TZVPP (in Parentheses) Level of Theory

	PA[a]			E_{BH_3}[b]			$E_{W(CO)_5}$[c]		
X	**2X**	**3X**	**8X**	**4X**	**5X**	**9X**	**6X**	**7X**	**10X**
C	250.1 (249.1)	228.6 (229.4)	361.2 (359.9)	−57.6	−16.0	−70.9	−9.5	20.7	14.3
Si	208.8 (212.0)	239.9 (241.7)	331.7 (334.5)	−33.3	−18.3	−48.4	−3.1	18.3	18.0
Ge	189.1 (190.7)	246.5 (248.8)	318.7 (321.0)	−21.6	−20.5	−38.9	7.2	16.1	26.6
Sn	174.9 (172.3)	254.3 (257.3)	315.1 (314.9)	−12.9	−22.9	−33.2	14.9	13.3	30.9

[a]PA is the proton affinity of **1X** at X and at C4 for the formation of monoprotonated products **2X** and **3X** and diprotonated product **8X**. [b]E_{BH3} is the energy for the reaction of BH_3 with **1X** at X and at C4 for the formation of mono-BH_3 adducts **4X** and **5X** and di-BH_3 adduct **9X**. [c]$E_{W(CO)5}$ is the reaction energy for **1X** + $W(CO)_6$ → **6X**/**7X** + CO and **1X** + 2$W(CO)_6$ → **10X** + 2CO.

on C1−C2−C3−C4 skeleton (named as "butadiene-type π−MO" in the subsequent discussion) which is antibonding between C2 and C3 with a small contribution from N atoms. The HOMO-1 is a lone pair on the carbene carbon atom and HOMO-2 is the π−MO having a nodal plane through two C−N bonds. The MOs of **1X** (where X = Si, Ge, and Sn) are similar to **1C** and the correlation diagram connecting these MOs of **1X** are plotted in Figure 2. The HOMO and HOMO-2 destabilizes when X changes from C to Sn, because of improper π-overlap of the $2p_z$ orbital on N atom with heavier Group 14 elements. On the other hand, the lone-pair MO (HOMO-1) stabilizes from **1C** to **1Sn**, which is attributed to the inertness of the lone pair, because of poor sp mixing in the heavier Group 14 elements.[15] The HOMO (−4.92 eV) and HOMO-1 (−5.00 eV) of **1C** are very close in energy. The lone-pair type molecular orbital becomes HOMO-2 for **1Ge** and **1Sn**. This indicates that the nucleophilicity at X gradually reduces and that at the C3−C4 exocyclic π-bond gradually increases when X changes from C to Sn.

The Wiberg bond indices and NBO charge analysis of **1X** are given in Table 1. The significantly less bond order for C2−C3, compared to C1−C2 and C3−C4, supports the butadiene-type nature of the C1−C2−C3−C4 fragment for **1X**. The NBO charge analysis shows a negative charge of approximately −0.5e on C4 atom for all **1X** and positive charge on X. The value of the positive charge on X for **1C** is only +0.13e, whereas the charge at X increases to approximately +1.00e for **1Si**−**1Sn**. Correspondingly, the negative charges on N1 and N2 is higher for **1Si**−**1Sn**. The partial occupancies in the s-orbital on X increase gradually from **1C** to **1Sn**, whereas that in the in-plane p-orbital reduces, indicating the reluctance for sp mixing.[15] This variation in partial occupancies can be correlated with the reduction of N1−X−N2 bond angle from 111.5° (**1C**) to 88.4° (**1Sn**). The negative charge on CH_2 group (between −0.09e and −0.13e) suggests that the C3−C4 π-bond is less polarized and it can be best described by the resonating structure $\mathbf{1X}_a$ with a minor (∼9%−13%) contribution from $\mathbf{1X}_b$, by considering the fact that a 100% polarization would lead to negative charge of −1.0e on CH_2 group. The Mulliken atomic and group charge distributions were also calculated (Table S3). The variations in the group charges are minimal, while the atomic charges vary significantly. Therefore, the qualitative description for the degree of polarization of C3−C4 π-bond obtained from the NBO group charge analysis will remain the same. This charge analysis is well complemented with positive NICS values and geometrical parameters.

Reactivity of 1X toward Proton, BH_3 and Complexation with $W(CO)_5$. The geometrical and bonding analysis on **1X** suggests two important Lewis basic positions, which are not a part of the π-delocalization in the six-membered ring, viz., the

dx.doi.org/10.1021/ic300821r | Inorg. Chem. 2012, 51, 8265−8274

Table 3. Calculated NICS Values at 1 Å above the Center of the Ring, NICS(1), Its Dissected NICS(1)$_{zz}$ (Shown in Parentheses), and NBO Group Charges (q) of CH_2/CH_2A at the BP86/TZVPP Level of Theory

X	2X	3X	4X	5X	6X	7X	8X	9X	10X
					NICS(1)[a] (NICS(1)zz)				
C	5.3 (17.6)	−7.8 (−19.8)	2.0 (8.1)	−3.5 (−7.5)	2.4 (10.2)	−1.6 (−2.4)	−7.6 (−20.1)	−2.4 (−4.5)	−0.6 (−0.4)
Si	4.3 (15.4)	−4.8 (−12.2)	1.8 (7.6)	−2.2 (−4.4)	2.1 (9.0)	−0.8 (−0.5)	−4.9 (−11.5)	−1.3 (−1.4)	0.0 (2.4)
Ge	6.2 (22.2)	−4.7 (−11.6)	2.4 (10.2)	−2.7 (−5.5)	2.6 (9.9)	−1.0 (−0.9)	−5.2 (−11.4)	−1.6 (−1.8)	−0.1 (2.3)
Sn	16.1 (52.3)	−3.8 (−8.6)	3.2 (13.1)	−2.1 (−3.2)	3.6 (14.5)	6.1 (21.9)	−4.3 (−8.1)	−1.5 (−1.1)	0.0 (1.3)
					q(CH_2/CH_2A)[b]				
C	0.09	0.13	−0.05	−0.48	−0.04	−0.37	0.23	−0.42	−0.29
Si	0.08	0.10	−0.07	−0.53	−0.06	−0.42	0.21	−0.47	−0.36
Ge	0.06	0.10	−0.08	−0.56	−0.08	−0.46	0.19	−0.51	−0.41
Sn	0.06	0.08	−0.11	−0.60	−0.10	−0.51	0.18	−0.57	−0.44

[a]For nonplanar molecules, NICS(1) and NICS(1)$_{zz}$ are at 1 Å from the center of the ring and away from group A (see Figure S1 in the Supporting Information). [b]A = H^+, BH_3 and $W(CO)_5$

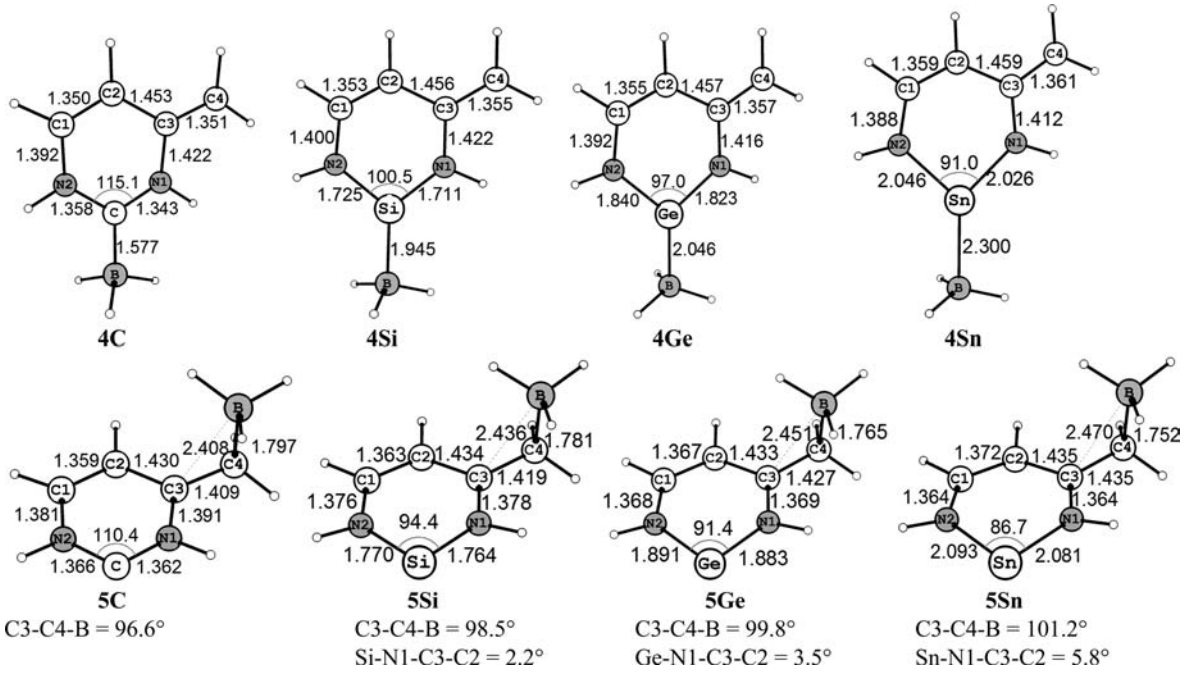

Figure 4. Optimized geometries (BP86/TZVPP) and important geometrical parameters of **4X** and **5X** (X = C, Si, Ge, and Sn). Distances are given in Ångstroms, angles are given in degrees.

lone pair at X and C4 atom or the C3−C4 π-bond. The protonated compounds and adducts with BH_3 and $W(CO)_5$ at X are represented by the structure numbers **2X**, **4X**, and **6X**, respectively, while the corresponding complexations at C4 are represented by the structure numbers **3X**, **5X**, and **7X**, respectively (Scheme 2).

Figure 3 shows the optimized protonated structures **2X** and **3X**. The six-membered rings of all the structures are planar except for **2Sn**. The C3−N1−N2−Sn angle is 161.2°, and the pyramidalization angle (θ_p), as defined by Haddon and co-workers,[28] is 8.9° around Sn. The geometrical parameters at the butadiene fragment (C1−C2−C3−C4) do not change considerably, compared to the parent systems **1X** (Figure 1). However, the X−N bond distances decrease and N1−X−N2 angle increases in **2X**. On the other hand, protonation at C4 leads to **3X**, where the C3−C4 bond distance elongated significantly as compared to **1X**. The C1−C2 and C2−C3 bond distances are almost in the same range 1.38−1.41 Å. There is significant reduction in the C−N bond distances and elongation in the X−N bond distances in **3X** as compared to parent systems. These geometrical data indicate greater delocalization in the six-membered ring of **3X**, compared to **1X** and **2X**.

The proton affinity values at X and C4 of **1X** are shown in Table 2. The proton affinities at the carbene carbon atom and at C4 are 250.1 (249.1) kcal/mol and 228.6 (229.4) kcal/mol, respectively, for **1C**. The values in parentheses are at the M06/TZVPP//BP86/TZVPP level of theory. Note that the proton affinity at X is higher than that at C4 for **1C** and a reverse trend is observed for heavier analogues. The difference between the proton affinity at X and C4 for **1C** is 21.5 (19.7) kcal/mol. This difference becomes −31.1 (−29.7) kcal/mol for **1Si**, −57.4 (−58.1) kcal/mol for **1Ge**, and −79.4 (−85.0) kcal/mol for **1Sn**. The gradual decrease in the proton affinity values at X indicates that the lone pair of electrons at X becomes less available when X changes from C to Sn. This can be interpreted from the gradual stabilization of the lone-pair type MOs for **1C**−**1Sn** (Figure 2). Similarly, the increase in the proton

dx.doi.org/10.1021/ic300821r | Inorg. Chem. 2012, 51, 8265−8274

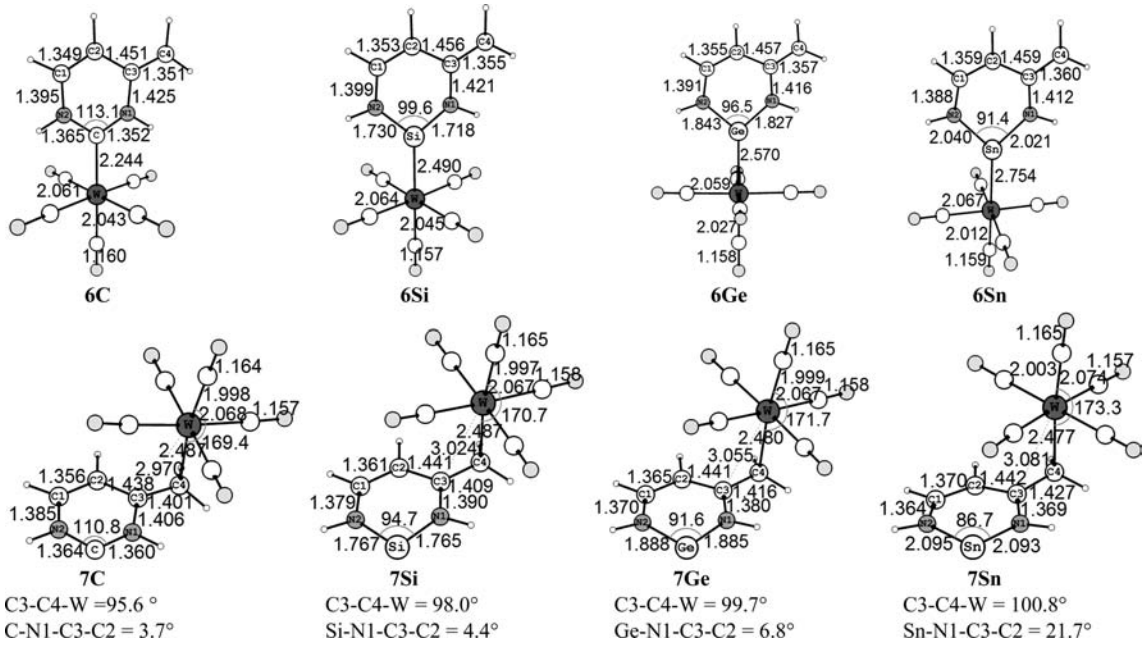

Figure 5. Optimized geometries (BP86/TZVPP) and important geometrical parameters of **6X** and **7X** (X = C, Si, Ge, and Sn). Distances are given in Ångstroms, angles are given in degrees.

affinity values at C4 can be correlated with the increasing destabilization of the butadiene type π-MO from **1C** to **1Sn**. On the other hand, the proton affinity of NHC is 254.2 kcal/mol at the BP86/TZVPP//BP86/SVP level of theory,[29] which is comparable to the proton affinity of **1C** at X (250.1 kcal/mol). It is noteworthy that the proton affinities of **1X** at C4 are much higher than that of ethylene (162.7 kcal/mol) at the same level of theory. The higher proton affinity at C4 indicates higher tendency for the polarization of the exocyclic C3−C4 π-bond, leading to a resonating structure **1X**$_b$, (see Scheme 2). This polarization via protonation helps to attain aromaticity in the six-membered ring, which is adequately reflected in the negative NICS(1) and NICS(1)$_{zz}$ values (see Table 3). The NICS values reduce from **3C** to **3Sn**. On the other hand, the NICS values for **2X** are positive and higher than those of the parent systems. The exceptionally high NICS values for **2Sn** can be attributed to a nonplanar geometry.

The bond orders of C1−C2, C2−C3 and C3−C4 for **2X** are closer to **1X** (see Table 1 and Table S2 in the Supporting Information). On the contrary, the bond orders of C1−C2 and C2−C3 are comparable for **3X** and lie within the range of 1.35−1.48 and the bond order for C3−C4 reduces, compared to **1X**. The NBO charge analysis shows that the positive charge on X increases substantially for **2X**, compared to **3X**. The positive charge of 0.09−0.06e on CH_2 group in **2X** suggests that the C3−C4 bond is less polarized (~9%−6%) by considering the fact that 100% polarization would lead to a charge of −1.0e on the CH_2 group (see Table 3). Interestingly, the protonation increases the negative charge on C4 in **3X**, while a slight reduction in the negative charge is noted for **2X**. This is a clear indication of the polarization of the C3−C4 π-bond toward C4 for **3X**, which is well supported by the negative NICS values. Similar group charge analysis on **3X** implies very high (~87%−92%) polarization of the C3−C4 π-bond.

These data clearly support that both Lewis basic positions, viz., X and C4 of the six-membered carbene and its heavier analogues, are highly accessible toward protonation and their relative reactivity can be understood from the energetics of the proton affinity discussed earlier. Even though **1X** is non-aromatic in nature, the controlled and targeted protonation can lead either to the aromatic system **3X** having a lone pair on X or the nonaromatic system **2X** having a readily polarizable C3−C4 π-bond.

In order to further explore the Lewis basic character at X and C4, we have studied the reaction of **1X** with BH_3 and $W(CO)_6$ (see Scheme 2). The addition of BH_3 at X changes the geometrical parameters in a similar fashion as that of the protonated analogues **2X**, but to a lesser extent (see Figure 4). Note that **4Sn** is planar in contrast to nonplanar **2Sn**. The C3−C4−B bond angles of **5X** are in the range of 96.6°−101.2°. The shorter C3−C4 and C1−C2 bond distances as well as the longer C2−C3 bond distance, compared to **3X**, indicate that the C3−C4 π-bond is less polarized toward BH_3 than H^+. The C4−B bond distances are in the range of 1.80−1.75 Å, while the C3−B bond distances are in the range of 2.41−2.47 Å. The longer C3−B bond distances indicate a semibridging nature of the BH_3 group and the highly polarizable C3−C4 π-bond in **1X**. It is interesting to note that the addition of BH_3 to ethylene π-bond leads to B−H bond breaking and forms $CH_3CH_2BH_2$ at the same level of theory. In contrast, BH_3 could polarize the C3−C4 π-bond in **1X** and forms the semibridged BH_3 adduct **5X**. Note that **5Si**, **5Ge**, and **5Sn** are nonplanar. The Si−N1−C3−C2 dihedral angle is 2.2°, the Ge−N1−C3−C2 dihedral angle is 3.5° and the Sn−N1−C3−C2 dihedral angle is 5.8°.

The reaction energies (E_{BH3}) for the formation of **4X** and **5X** from **1X** are given in Table 2.[30] All the reactions are exothermic and show a similar trend, like protonation (viz-a-viz, the reaction energy gradually decreases for **4X** and increases for **5X** when X changes from C to Sn). However, in contrast to the proton affinity, the reaction energy for **1X** + BH_3 → **4X** is more exothermic than **1X** + BH_3 → **5X** for X = C and Si. **1Ge** shows very close energetics for the above two reactions. The reverse order is noted only for **1Sn**, which implies that the lone pair on

dx.doi.org/10.1021/ic300821r | Inorg. Chem. 2012, 51, 8265−8274

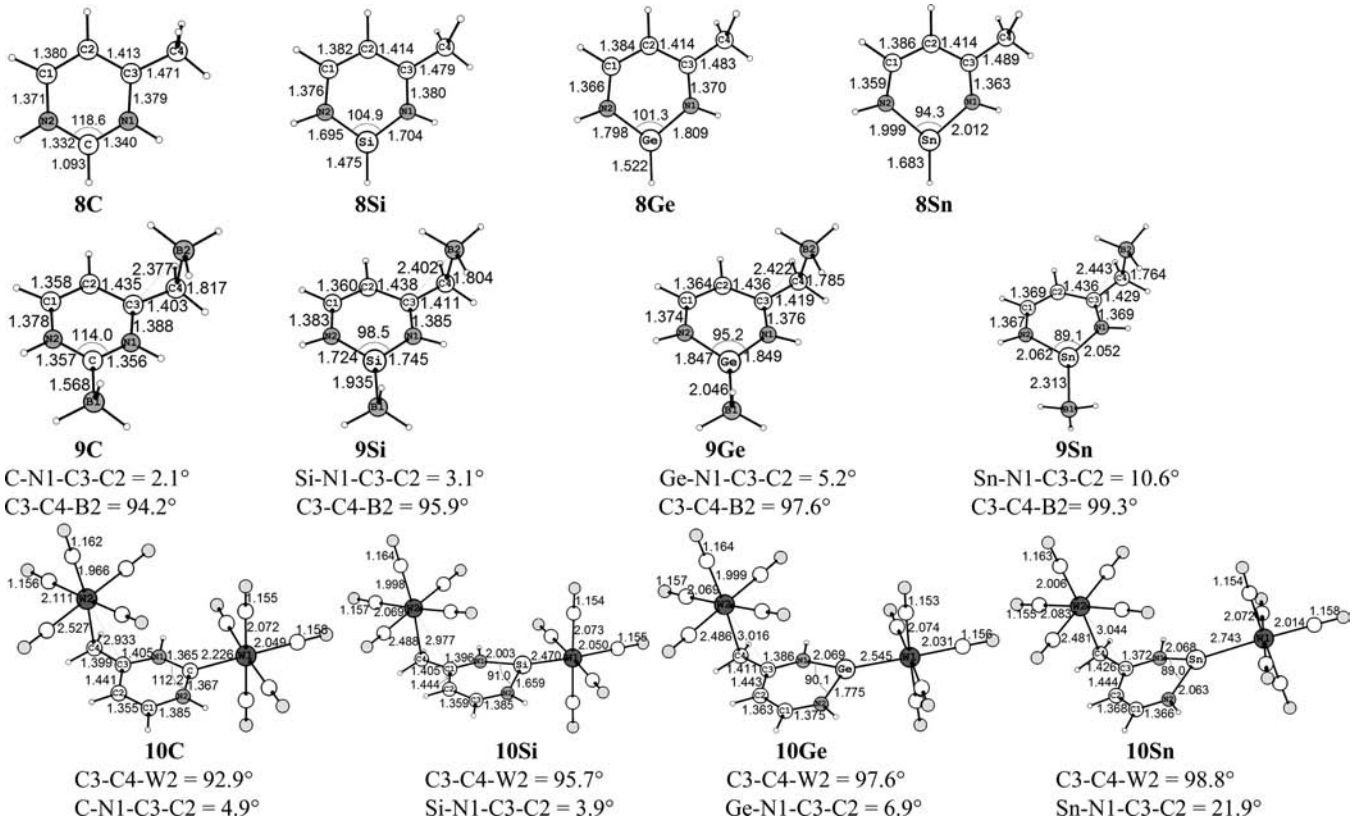

Figure 6. Optimized geometries (BP86/TZVPP) and important geometrical parameters of **8X, 9X**, and **10X** (X = C, Si, Ge, and Sn). Distances are given in Ångstroms, angles are given in degrees.

Sn is rather inert toward the reaction with BH_3. The formation of a stronger C−H bond, compared to the C−B bond, also contributes toward the reaction energy. The reaction energy for the formation of BH_3 adduct with five-membered NHC is −58.6 kcal/mol at the BP86/TZVPP//BP86/SVP level of theory, which is comparable to our calculated data for **1C** (−57.6 kcal/mol).[29b] Similar to **3X**, the addition of BH_3 at C4 renders aromatic character into the ring, as indicated by the negative NICS values for **5X** (see Table 3). The shorter C3−C4 bond distance and higher bond order in **5X**, compared to **3X**, supports this (see Table S2 in the Supporting Information). The NICS values for **4X** are positive indicating nonaromatic localized geometry similar to that of **1X** and **2X**. Analysis of CH_2 group charges (between −0.05e and −0.11e) in **4X** indicates slight polarization (∼5%−11%) of the C3−C4 π-bond (see Table 3). Similarly, the negative CH_2BH_3 group charges (from −0.48e to −0.60e) in **5X** implies moderate (∼48%−60%) polarization of the C3−C4 π-bond. The effect of polarization of the C3−C4 π-bond by BH_3 is significantly less than the polarization by H^+. However, both Lewis basic sites are available for coordination with BH_3.

The optimized geometries of **6X** and **7X** are shown in Figure 5. The changes in the geometrical parameters of butadiene fragments (C1−C2−C3−C4) of **6X** are similar to that of **2X** and **4X**. The coordination of C4 to $W(CO)_5$ also leads to a semibridging structure **7X** as that of **5X**. Even though the extent of nonplanarity in **7X** is more, other geometrical parameters do not change considerably in comparison to **5X**. The major geometrical changes are observed in the X−N1−C3−C2 dihedral angle, which can be attributed to the bulky $W(CO)_5$ fragment. The C3−W bond distances are in the range of 2.97−3.08 Å, the C4−W bond distances are ∼2.48 Å, and C3−C4−W angles are in the range of 96.6°−100.8° in **7X**. The less polarization of C3−C4 π-bond, compared to **3X**, is reflected in the shorter C3−C4 and C1−C2 bond distances as well as the longer C2−C3 bond distances. The corresponding bond orders and NBO charges support this observation (see Table S2 in the Supporting Information). However, the effect is marginally smaller than that in **5X**.

The reaction of **1X** with $W(CO)_6$ (**1X** + $W(CO)_6$ → **6X** + CO and **1X** + $W(CO)_6$ → **7X** + CO, Scheme 2) is less favorable, compared to the reaction with BH_3 (Table 2). All the complexation energies are endothermic, except for the formation of **6C** and **6Si**. Note that this complexation energy is compared to that of the stronger ligand CO. In this context, the exothermicity of the reactions of **1C** and **1Si** with $W(CO)_6$ demonstrates them as stronger ligands than CO for the complexation reaction with transition-metal fragment $W(CO)_5$. It is interesting to note that the corresponding complexation energies of ligands such as five-membered NHC and ethylene with $W(CO)_6$ are only −9.9 and 17.5 kcal/mol, respectively, at the same level of theory. This suggests that both X and C3−C4 π-bond of **1X** could be accessible for complexation with metal fragments. The energy required for the dissociation of the NHC-$W(CO)_5$ into NHC and $W(CO)_5$ is 58.6 kcal/mol at the BP86/TZVPP//BP86/SVP levels of theory.[29b] The corresponding dissociation energy for **6C** is 52.1 kcal/mol, which suggests that the coordinating ability of the carbene carbon atom in **1C** is similar to that of NHC. Although **7X** compounds are nonplanar, the negative NICS values for **7C**−**7Ge** support our description of a polarized C3−C4 π-bond (see Table 3). The higher degree of nonplanarity in **7Sn** is reflected in the

dx.doi.org/10.1021/ic300821r | Inorg. Chem. 2012, 51, 8265−8274

corresponding positive NICS values. Analysis of the CH_2 group charges (between −0.04e and −0.10e) in **6X** indicates slight (∼4%−10%) polarization of the C3−C4 π-bond (see Table 3). Similarly, the negative $CH_2W(CO)_5$ group charges (between −0.37e and −0.51e) in **7X** suggests moderate (∼37%−51%) polarization of the C3−C4 π-bond. The effect of polarization of the C3−C4 π-bond by $W(CO)_5$ is comparable to BH_3 but significantly less than the polarization by H^+.

Reactivity of 1X toward Two Lewis Acids (H^+, BH_3, and $W(CO)_5$). The concurrent reactivity of the lone pair on X and the C3−C4 π-bond in **1X** was examined by the reactions with two Lewis acids. The optimized geometries of the diprotonated compounds and diadducts with BH_3 and $W(CO)_5$ at both the Lewis basic positions are represented by structure numbers **8X**, **9X**, and **10X**, respectively (see Figure 6).

The diprotonated **8X** renders intermediate geometrical parameters, compared to **2X** and **3X** (see Figure 3). Note that the geometrical parameters of the butadiene (C1−C2−C3−C4) fragment are close to those of **3X**, whereas that of the diaminocarbene (N1−X−N2) fragment is close to **2X**. The Wiberg bond order data are also in accordance with the geometrical parameters (see Table S2 in the Supporting Information). The first and second PA values for **1X** are calculated as follows. The highest mono protonation energy of **1X** is considered as the first PA. The difference between the double protonation energy (see Table 2) and first PA gives the respective second PA. The first protonation occurs at the carbene carbon atom in **1C** and at C4 in **1Si**−**1Sn**. The first PA values for **1X** are in the range of 239.9−254.3 kcal/mol, while the second PAs are in the range of 60.8−111.1 kcal/mol, and it decreases from **1C** to **1Sn**. It is interesting to note that the lone pair on heavier elements show reluctance toward donation, as indicated by lower values of second PA. The group charge analysis by NBO shows that the C3−C4 π-bond in **8X** is slightly less (∼77%−82%) polarized than in **3X** (see Table 3). However, this amount of polarization of the C3−C4 π-bond is sufficient to introduce aromatic delocalization into the six-membered ring, as observed by the negative NICS(1) and $NICS(1)_{zz}$ values.

The six-membered ring in **9X** is nonplanar and the nonplanarity increases from **9C** to **9Sn** (see Figure 6). The semibridging nature of the BH_3 attached at C4 observed in **5X** is also retained in **9X**, as indicated by the C3−C4−B2 angles (94.2°−99.3°) as well as the longer C3−B2 bond distances (2.337−2.443 Å). As observed in **8X**, the geometrical parameters and the Wiberg bond indices of **9X** show similar trends, viz., the butadiene unit is close to **5X** and the diaminocarbene part is close to **4X**. The reaction energy for the formation of **9X** from **1X** is exothermic (see Table 2) and reduces from **1C** to **1Sn**. It is noteworthy that the reaction energy for the formation of diadducts with BH_3 (E_{BH3} for **9X**) is approximately the additive reaction energies for the formation of monoadducts (E_{BH3} for **4X** + E_{BH3} for **5X**) with an average deviation of ∼2.9 kcal/mol. Thus, the reaction at one of the Lewis basic positions in **1X** does not significantly alter the reactivity of the other. On the other hand, Driess and co-workers reported that the heavier Group 14 elements act as an electrophile toward OTf^- upon the addition of a Lewis acid to the exocyclic CH_2 group.[9,10a] However, the exothermicity of the reactions indeed suggests both X and the C3−C4 π-bond are available concurrently for the reaction with Lewis acids. The polarization of the C3−C4 π-bond in **9X** (∼42%−57%), based on NBO group charge analysis, is much closer to **5X** (∼48%−60%) (see Table 3). However, the NICS(1) and $NICS(1)_{zz}$ values are close to zero, which is attributed to the nonplanarity of the six-membered ring in **9X**.

The characteristic in the geometrical variations noted for **9X** are similar for **10X** as well. The reaction energies for **1X** + $2W(CO)_6$ → **10X** + 2CO are endothermic and increases from **10C** to **10Sn**. In this case, the reaction energy for the formation of diadducts with $W(CO)_6$ ($E_{W(CO)5}$ for **10X**) also is approximately the additive reaction energies for the formation of monoadducts ($E_{W(CO)5}$ for **6X** + $E_{W(CO)5}$ for **7X**) with an average deviation of ∼3.0 kcal/mol. Consequently, the reaction at one of the Lewis basic positions in **1X** does not significantly alter the reactivity of the other. The polarization of the C3−C4 π-bond calculated by NBO group charge is less (∼29%−44%) than **7X** (∼37%−51%) and the NICS(1) and $NICS(1)_{zz}$ values for **10X** shows nonaromatic character.

CONCLUSIONS

Computational quantum mechanical calculations on the six-membered N-heterocyclic carbene and its heavier analogues (**1X** (X = C, Si, Ge, and Sn)) having an exocyclic double bond at the C3 carbon atom have been carried out at the BP86 level of theory with TZVPP basis set to explore their electronic structure and reactivity of the lone pair versus the exocyclic double bond. **1X** can be represented by two resonating structures, viz., the nonaromatic localized structure $\mathbf{1X}_a$ and the delocalized structure $\mathbf{1X}_b$, with polarized exocyclic C3−C4 π-bond. The geometrical parameters, NICS values and NBO population analysis indicate that **1X** can be best described as $\mathbf{1X}_a$ with a minor contribution from $\mathbf{1X}_b$. The carbene carbon atom shows higher proton affinity for **1C**, whereas the exocyclic C4 atom shows higher proton affinity for heavier analogues. The aromatic stabilization energy gained by protonating the exocyclic double bond is higher than the reactivity of the lone pair on heavier Group 14 elements. The energetics for the diadduct formation with BH_3 and $W(CO)_5$ show that the reaction at one of the Lewis basic positions does not affect the reactivity of the other considerably. The protonation and adduct formation with BH_3 and $W(CO)_5$ at X lead to nonaromatic systems, whereas similar reactions at C4 lead to aromatic systems due to π-bond polarization at C3−C4. The maximum polarization of the C3−C4 π-bond is obtained for protonation.

ASSOCIATED CONTENT

Supporting Information

Table S1 with the Cartesian coordinates and the total electronic energies of the calculated molecules, Table S2 with the NBO bond orders and atomic charges, Table S3 with the Mulliken atomic and group charges, Table S4 with the NICS values, Table S5 with the reaction energy for the reaction of **1X** with B_2H_6, and Figure S1 with the schematic representation of the choice of points at which NICS values are calculated. This material is available free of charge via the Internet at http://pubs.acs.org.

AUTHOR INFORMATION

Corresponding Author

*Tel.: 0091-495-228-5304. Fax: 0091-495-228-7250. E-mail: param@nitc.ac.in.

Notes

The authors declare no competing financial interest.

■ ACKNOWLEDGMENTS

V.C.R. thanks MHRD for research fellowship and P.P. thanks FRG research grant (Grant No: FRG10-11/0104) from NIT Calicut. Excellent service by the computer center of NIT Calicut is gratefully acknowledged. Authors sincerely thank reviewers for their valuable comments for improving the manuscript.

■ REFERENCES

(1) (a) Moss, R. A.; Platz, M. S.; Jones, M. Jr., Eds. *Reactive Intermediates Chemistry*; John Wiley & Sons: New York, 2004. (b) Arduengo, A. J., Bertrand, G., Eds. *Chem. Rev.* **2009**, *109* (8) (Special Issue on Carbenes; entire issue). (c) Denmark, S. E.; Beutner, G. L. *Angew. Chem., Int. Ed.* **2008**, *47*, 1560−1638. (d) Kamber, N. E.; Jeong, W.; Waymouth, R. M.; Pratt, R. C.; Lohmeijer, B. G. G.; Hedrick, J. L. *Chem. Rev.* **2007**, *107*, 5813−5840. (e) Frey, G. D.; Lavallo, V.; Donnadieu, B.; Schoeller, W. W.; Bertrand, G. *Science* **2007**, *316*, 439−441. (f) Alcarazo, M.; Lehmann, C. W.; Anoop, A.; Thiel, W.; Fűrstner, A. *Nat. Chem.* **2009**, *1*, 295−301. (g) Aldeco-Perez, E.; Rosenthal, A. J.; Donnadieu, B.; Parameswaran, P.; Frenking, G.; Bertrand, G. *Science* **2009**, *326*, 556−559. (h) Benhamou, L.; Chardon, E.; Lavigne, G.; Bellemin-Laponnaz, S.; César, V. *Chem. Rev.* **2011**, *11*, 2705−2733. (i) Gierz, V.; Maichle-Mössmer, C.; Kunz, D. *Organometallics* **2012**, *31*, 739−747. (j) Grubbs, R. H. *Angew. Chem., Int. Ed.* **2006**, *45*, 3760−3765. (k) Marion, N.; Diez-Gonzalez, S.; Nolan, S. P. *Angew. Chem., Int. Ed.* **2007**, *46*, 2988−3000. (l) Enders, D.; Niemeier, O.; Henseler, A. *Chem. Rev.* **2007**, *107*, 5606−5655. (m) Tonner, R.; Frenking, G. *Angew. Chem., Int. Ed.* **2007**, *46*, 8695−8698. (n) Back, O.; Donnadieu, B.; Parameswaran, P.; Frenking, G.; Bertrand, G. *Nat. Chem.* **2010**, *2*, 369−373. (o) Martin, D.; Melaimi, M.; Soleilhavoup, M.; Bertrand, G. *Organometallics* **2011**, *30*, 5304−5313. (p) Arduengo, A. J.; Bertrand, G. *Chem. Rev.* **2009**, *109*, 3209−3210. (q) Nair, V.; Menon, R. S.; Biju, A. T.; Sinu, C. R.; Paul, R. R.; Jose, A.; Sreekumar, V. *Chem. Soc. Rev.* **2011**, *40*, 5336−5346. (r) Cabeza, J. A.; García-Álvarez, P. *Chem. Soc. Rev.* **2011**, *40*, 5389−5405. (s) Biju, A. T.; Kuhl, N.; Glorius, F. *Acc. Chem. Res.* **2011**, *44*, 1182−1195.

(2) (a) Igau, A.; Grutzmacher, H.; Baceiredo, A.; Bertrand, G. *J. Am. Chem. Soc.* **1988**, *110*, 6463−6466. (b) Igau, A.; Baceiredo, A.; Trinquier, G.; Bertrand, G. *Angew. Chem., Int. Ed.*. **1989**, *28*, 621−622. (c) Ritter, S. K. *Chem. Eng. News* **2012**, *90*, 34−36. (d) Arduengo, A. J., III; Harlow, R. L.; Kline, M. *J. Am. Chem. Soc.* **1991**, *113*, 361−363.

(3) Denk, M.; Lennon, R.; Hayashi, R.; West, R.; Belyakov, A. V.; Verne, H. P.; Haaland, A.; Wagner, M.; Metzler, N. *J. Am. Chem. Soc.* **1994**, *116*, 2691−2692.

(4) Herrmann, W. A.; Denk, M.; Behm, J.; Scherer, W.; Klingan, F. R.; Bock, H.; Solouki, B.; Wagner, M. *Angew. Chem., Int. Ed.* **1992**, *31*, 1485−1488.

(5) Gans-Eichler, T.; Gudat, D.; Nieger, M. *Angew. Chem., Int. Ed.* **2002**, *41*, 1888−1891.

(6) (a) Mansell, S. M.; Russel, C. A.; Wass, D. F. *Inorg. Chem.* **2008**, *47*, 11367−11375. (b) Charmant, J. P. H.; Haddow, M. F.; Hahn, F. E.; Heitmann, D.; Fröhlich, R.; Mansell, S. M.; Russell, C. A.; Wass, D. F. *Dalton Trans.* **2008**, 6055−6059.

(7) (a) Asay, M.; Jones, C.; Driess, M. *Chem. Rev.* **2011**, *111*, 354−396. (b) Mizuhata, Y.; Sasamori, T.; Tokitoh, N. *Chem. Rev.* **2009**, *109*, 3479−3511. (c) Boehme, C.; Frenking, G. *J. Am. Chem. Soc.* **1996**, *118*, 2039−2046. (d) Al-Rafia, S. M. I.; Malcolm, Adam C.; Liew, Sean K.; Ferguson, Michael J.; McDonald, R.; Rivard, E. *Chem. Commun.* **2011**, *47*, 6987−6989. (e) Heitmann, D.; Pape, T.; Hepp, A.; Mück-Lichtenfeld, C.; Grimme, S.; Hahn, F. E. *J. Am. Chem. Soc.* **2011**, *133*, 11118−11120. (f) Zabula, A. V.; Hahn, F. E. *Eur. J. Inorg. Chem.* **2008**, 5165−5179.

(8) (a) Bazinet, P.; Yap, G. P. A.; Richeson, D. S. *J. Am. Chem. Soc.* **2003**, *125*, 13314−13315. (b) Präsang, C.; Donnadieu, B.; Bertrand, G. *J. Am. Chem. Soc.* **2005**, *127*, 10182−10183. (c) Krahulic, K. E.; Tuononen, H. M.; Parvez, M.; Roesler, R. *J. Am. Chem. Soc.* **2009**, *131*, 5858−5865. (d) Iglesias, M.; Beetstra, D. J.; Knight, J. C.; Ooi, L.-L.; Stasch, A.; Coles, S.; Male, L.; Hursthouse, M. B.; Cavell, K. J.; Dervisi, A.; Fallis, I. A. *Organometallics* **2008**, *27*, 3279−3289. (e) Kolychev, E. L.; Portnyagin, I. A.; Shuntikov, V. V.; Khrustalev, V. N.; Nechaev, M. S. *J. Organomet. Chem.* **2009**, *694*, 2454−2462. (f) Alder, R. W.; Blake, M. E.; Bortolotti, C.; Bufali, S.; Butts, C. P.; Linehan, E.; Oliva, J. M.; Orpen, A. G.; Quayle, M. J. *Chem. Commun.* **1999**, 241−242. (g) Jazzar, R.; Liang, H.; Donnadieu, B.; Bertrand, G. *J. Organomet. Chem.* **2006**, *691*, 3201−3205. (h) Makhloufi, A.; Frank, W.; Ganter, C. *Organometallics* **2012**, *31*, 2001−2008. (i) Wang, R.-H.; Su, M.-D. *Organometallics* **2009**, *28*, 4324−4334. (j) Olah, J.; Veszpremi, T.; de Proft, F.; Geerlings, P. *J. Phys. Chem. A* **2007**, *111*, 10815−10823.

(9) Driess, M.; Yao, S.; Brym, M.; van Wüllen, C.; Lentz, D. *J. Am. Chem. Soc.* **2006**, *128*, 9628−9629.

(10) (a) Driess, M.; Yao, S.; Brym, M.; van Wüllen, C. *Angew. Chem., Int. Ed.* **2006**, *45*, 4349−4352. (b) Yao, S.; Xiong, Y.; Driess, M. *Organometallics* **2011**, *30*, 1748−1767.

(11) (a) Percival, P. W.; McCollum, B. M.; Brodovitch, J.-C.; Driess, M.; Mitra, A.; Mozafari, M.; West, R.; Xiong, Y.; Yao, S. *Organometallics* **2012**, *31*, 2709−2714. (b) Szilvási, T.; Nyíri, K.; Veszprémi, T. *Organometallics* **2011**, *30*, 5344−5351.

(12) (a) Wang, W.; Inoue, S.; Yao, S.; Driess, M. *Organometallics* **2011**, *30*, 6490−6494. (b) Yao, S.; Zhang, X.; Xiong, Y.; Schwarz, H.; Driess, M. *Organometallics* **2010**, *29*, 5353−5357.

(13) Nyiri, K.; Veszprémi, T. *Organometallics* **2009**, *28*, 5909−5914.

(14) (a) Amani, J.; Musavi, S. M. *Tetrahedron* **2011**, *67*, 749−754. (b) Wang, R.-H.; Su, M.-D. *J. Phys. Chem. A* **2008**, *112*, 7689−7698.

(15) (a) Kaupp, M.; Schleyer, P. v. R. *J. Am. Chem. Soc.* **1993**, *115*, 1061−1073. (b) Power, P. P. *Chem. Rev.* **1999**, *99*, 3463−3503.

(16) (a) Becke, A. D. *Phys. Rev. A* **1988**, *38*, 3098−3100. (b) Perdew, J. P. *Phys. Rev. B* **1986**, *33*, 8822−8824. (c) Perdew, J. P. *Phys. Rev. B* **1986**, *34*, 7406−7406.

(17) Weigend, F.; Ahlrichs, R. *Phys. Chem. Chem. Phys.* **2005**, *7*, 3297−3303.

(18) (a) Fan, L.; Ziegler, T. *J. Chem. Phys.* **1992**, *96*, 9005−9012. (b) Fan, L.; Ziegler, T. *J. Phys. Chem.* **1992**, *96*, 6937−6941.

(19) Frisch, M. J.; Trucks, G. W.; Schlegel, H. B.; Scuseria, G. E.; Robb, M. A.; Cheeseman, J. R.; Scalmani, G.; Barone, V.; Mennucci, B.; Petersson, G. A.; Nakatsuji, H.; Caricato, M.; Li, X.; Hratchian, H. P.; Izmaylov, A. F.; Bloino, J.; Zheng, G.; Sonnenberg, J. L.; Hada, M.; Ehara, M.; Toyota, K.; Fukuda, R.; Hasegawa, J.; Ishida, M.; Nakajima, T.; Honda, Y.; Kitao, O.; Nakai, H.; Vreven, T.; Montgomery, Jr., J. A.; Peralta, J. E.; Ogliaro, F.; Bearpark, M.; Heyd, J. J.; Brothers, E.; Kudin, K. N.; Staroverov, V. N.; Kobayashi, R.; Normand, J.; Raghavachari, K.; Rendell, A.; Burant, J. C.; Iyengar, S. S.; Tomasi, J.; Cossi, M.; Rega, N.; Millam, N. J.; Klene, M.; Knox, J. E.; Cross, J. B.; Bakken, V.; Adamo, C.; Jaramillo, J.; Gomperts, R.; Stratmann, R. E.; Yazyev, O.; Austin, A. J.; Cammi, R.; Pomelli, C.; Ochterski, J. W.; Martin, R. L.; Morokuma, K.; Zakrzewski, V. G.; Voth, G. A.; Salvador, P.; Dannenberg, J. J.; Dapprich, S.; Daniels, A. D.; Farkas, Ö.; Foresman, J. B.; Ortiz, J. V.; Cioslowski, J.; Fox, D. J. Gaussian 09, Revision B.1; Gaussian, Inc.: Wallingford, CT, 2009.

(20) (a) Reed, A. E.; Curtiss, L. A.; Weinhold, F. *Chem. Rev.* **1988**, *88*, 899−926. (b) Glendening, E. D.; Reed, A. E.; Carpenter, J. E.; Weinhold, F. NBO Version 5.9.

(21) (a) Schleyer, P. v. R.; Maerker, C.; Dransfeld, A.; Jiao, H.; Hommes, N. J. R. v. E. *J. Am. Chem. Soc.* **1996**, *118*, 6317−6318. (b) Chen, Z.; Wannere, C. S.; Corminboeuf, C.; Puchta, R.; Schleyer, P. v. R. *Chem. Rev.* **2005**, *105*, 3842−3888. (c) Schleyer, P. v. R.; Manoharan, M.; Wang, Z. X.; Kiran, B.; Jiao, H. J.; Puchta, R.; Hommes, N. J. R. v. E. *Org. Lett.* **2001**, *3*, 2465−2468. (d) Badri, Z.; Foroutan-Nejad, C.; Rashidi-Ranjbar, P. *Phys. Chem. Chem. Phys.* **2012**, *14*, 3471−3481.

(22) Wolinski, K.; Hinton, J. F.; Pulay, P. *J. Am. Chem. Soc.* **1990**, *112*, 8251−8260.

(23) Rappoport, D.; Furche, F. *J. Chem. Phys.* **2010**, *133*, 134105.

(24) Zhao, Y.; Truhlar, D. G. *Theor. Chem. Acc.* **2008**, *120*, 215−241.

(25) The bond lengths of *trans*-butadiene at BP86/TZVPP level of theory are: d(C1−C2), d(C3−C4) = 1.345 Å; d(C2−C3) = 1.453 Å.

(26) Guha, A. K.; Sarmah, S.; Phukan, A. K. *Dalton Trans.* **2010**, *39*, 7374−7383.
(27) The HOMO−LUMO gap decreases from **1C** to **1Sn**, viz., 3.08 eV for **1C**, 2.49 eV for **1Si**, 1.98 eV for **1Ge** and 1.42 eV for **1Sn**. The corresponding values, however, are slightly higher for the five-membered NHC (4.66 eV) and its heavier Si (3.45 eV), Ge (2.96 eV) and Sn (2.26 eV) analogues.
(28) (a) Haddon, R. C. *J. Phys. Chem. A* **2001**, *105*, 4164−4165. (b) Haddon, R. C.; Chow, S. Y. *J. Am. Chem. Soc.* **1998**, *120*, 10494−10496.
(29) (a) Tonner, R.; Heydenrych, G.; Frenking, G. *Chem. Phys. Chem.* **2008**, *9*, 1474−1481. (b) Tonner, R.; Heydenrych, G.; Frenking, G. *Chem.−Eur. J.* **2008**, *14*, 3273−3289.
(30) The energetics for the reaction of **1X** with B_2H_6 (2 **1X** + B_2H_6 → 2 **4X**/**5X**) were calculated at the BP86/TZVPP level of theory (see Table S5 in the Supporting Information). The trends in energetics are similar to that of the reaction with BH_3 (see Table 2). The reaction is exothermic for the formation of **4C**-**4Ge** and **5Sn**. The endothermicity for the other products can be attributed to the dissociation energy of B_2H_6 into two BH_3, which is 41.1 kcal/mol.